

**Purdue University**  
**Purdue e-Pubs**

---

International Compressor Engineering Conference

School of Mechanical Engineering

---

1996

# Mathematical Modelling of Radial and Non-Radial Rotary Sliding Vane Compressors

A. B. Tramschek  
*University of Strathclyde*

M. H. Mkumbwa  
*University of Dar Es Salaam*

Follow this and additional works at: <https://docs.lib.purdue.edu/icec>

---

Tramschek, A. B. and Mkumbwa, M. H., "Mathematical Modelling of Radial and Non-Radial Rotary Sliding Vane Compressors" (1996). *International Compressor Engineering Conference*. Paper 1151.  
<https://docs.lib.purdue.edu/icec/1151>

This document has been made available through Purdue e-Pubs, a service of the Purdue University Libraries. Please contact [epubs@purdue.edu](mailto:epubs@purdue.edu) for additional information.

Complete proceedings may be acquired in print and on CD-ROM directly from the Ray W. Herrick Laboratories at <https://engineering.purdue.edu/Herrick/Events/orderlit.html>

# MATHEMATICAL MODELLING OF RADIAL AND NON-RADIAL ROTARY SLIDING VANE COMPRESSORS

A. B. TRAMSCHEK  
Senior Lecturer  
Energy Systems Division  
Department of Mechanical Engineering  
University of Strathclyde  
Glasgow, Scotland

M. H. MKUMBWA  
Lecturer  
Department of Mechanical Engineering  
University of Dar Es Salaam  
Dar Es Salaam  
Tanzania

## ABSTRACT

A computer based model of a sliding vane air compressor was used to predict the behaviour of machines having different geometries operating at different conditions. The model was used to calculate the free air delivery, the required power input and a specific capacity defined as the free air delivery per unit of power input. Results from the modelling process were incorporated in an optimisation algorithm to predict that combination of dimensions which would achieve a given free air delivery at specified operating conditions and have optimum performance ( maximum specific capacity ).

The paper describes the simulation model developed to analyse the behaviour of both radial and non-radial vane sliding vane machines. Studies were performed to investigate the effects of varying both the number and the inclination of the vanes upon compressor performance at design and off design operating conditions.

Results are presented for a six vane machine having vane inclinations in the range  $-30^{\circ}$  to  $+30^{\circ}$ . The effect of varying the number of vanes upon compressor performance is also discussed.

## 1.0 INTRODUCTION

Ever since Ramelli first introduced the concept of multi-cell sliding vane devices in 1588 engineers and academics have sought to gain a greater appreciation of the subtleties of their operation and manufacturers have introduced design modifications which have improved significantly their performance and reliability. These activities continue today as energy conservation considerations and market forces compel manufacturers to produce even more reliable and efficient machines at competitive prices. In 1972, Peterson and McGahan [1] reported on aspects of sliding vane compressor behaviour. They commented on vane dynamics, vane friction, inter cell leakage, and the charging and the discharge processes. At the 1978 Purdue Compressor Technology Conference Pandeya and Soedel [2] described sliding and viscous friction models of relevance to sliding vane compressor design and discussed various leakage models. Sliding vane compressor studies at Strathclyde University were initiated in 1980 by Chang [3], continued from 1986 by Ooi [4], and taken further by Mkumbwa [5]. Chang developed a basic compressor simulation computer program and performed tests on a commercially available machine to verify his predictions. Ooi developed a more sophisticated model coupled with an optimisation algorithm to predict machine dimension combinations which would result in a machine having optimum performance defined as the maximum free air delivery per unit of power input. Ooi tested a purpose built prototype to corroborate his predictions. Mkumbwa's studies combined elements of Chang and Ooi's work but were extended to consider vane inclination and friction effects in greater detail. Some of Mkumbwa's experimental work is reported in a companion paper [6].

## 2.0 SIMULATION MODEL

The simulation model can be considered as comprising the following major elements:-

- a) Description of the compressor geometry.
- b) A thermodynamic analysis of the processes occurring in a typical working cell.
- c) A dynamic analysis of the vane behaviour including flank and tip friction effects.
- d) An analysis of bearing and end face friction effects.
- e) Use of an optimisation algorithm.

Elements a), b), c), d) are outlined in the following sections :-

### 2.1 Compressor Geometry.

The compressor geometry comprises a cylindrical rotor mounted eccentrically within a circular stator bore. Slots which house the sliding vanes are machined axially along the rotor at equal angular intervals around the rotor surface. The slots

may lie in a radial direction or be inclined in either a forward or a backward direction, see Figure 1 which illustrates the geometry for a forward inclined vane. During operation the vane tips are always assumed to be in contact with the stator surface. Constant size clearances are assumed to exist between the rotor and the stator in the sealing arc region, between the vane edges and the stator end plates, between the rotor end faces and the stator end plates, and between the rotor shaft and its bearing surfaces.

A working cell is formed by the region which exists between an adjacent pair of vanes, the cylindrical rotor and stator surfaces and the end plates. The variation of the size of this region as the rotor rotates forms the basis upon which the compressor operation depends. Suction and discharge ports are disposed at a number of locations on the stator surface. The cell angle  $\theta_c$  is defined as the angle formed by the lines which join the centre of the rotor to the points of contact of two adjacent vane tips on the stator surface. The motion of the vane is defined in terms of an angle  $\theta$  which represents the rotation of a line joining the centre of the rotor and the vane tip / stator surface contact point from a reference position known as Top Dead Centre (TDC). This concept is shown in Figure 1. The length of the line  $R_\theta$  represented by the distance OB in Figure 1 varies as a function of  $\theta$  according to :-

$$R_\theta = R_s \left( \sqrt{1 - a^2 \sin^2 \theta} - a \cos \theta \right) \dots\dots\dots(1.0)$$

where  $a = \varepsilon / R_s = (R_s - R_r) / R_s$

Inside the sealing arc,  $R_\theta = R_r + R_s$

For radial vanned machines, the time rate of change of  $\theta$  is constant and equal to the angular velocity of the rotor i.e

$$\frac{d\theta}{dt} = \omega = \text{constant} \dots\dots\dots(2.0)$$

For non-radial vanned machines, the line joining the centre of the rotor to the vane tip / stator surface contact point moves with a varying angular velocity. From Figure 1, it can be seen that :-

$$\theta = \rho + \psi + \phi + \zeta \dots\dots\dots(3.0)$$

differentiating the above expression but noting that since angle EOA is fixed for a given rotor so that  $\psi + \phi$  is constant then for non-radial vanned machines :-

$$\frac{d\theta}{dt} = \frac{d\rho}{dt} \pm \frac{d\zeta}{dt} = \omega \pm \frac{d\zeta}{dt} \dots\dots\dots(4.0)$$

Where the  $\pm$  sign applies depending whether there is a positive or a negative vane inclination. Thus unlike radial vane machines where the line joining the contact point to the rotor centre moves with a constant angular velocity and the cell angle is constant in non-radial vane machines both the cell angle and the angular velocity of the line joining the contact point to the rotor centre vary with time i.e with the angular position of the rotor see Figure 2 for an illustration of the way in which the cell angle  $\theta_c$  is defined. The variation of the cell angle  $\theta_c$  with angular position is shown in Figure 3.

## 2.2 Thermodynamic Considerations.

The cells defined by the geometry are treated in the simulation as small control volumes into which or from which working fluids may flow. The working fluids are the fluid which is being compressed and any agents e.g oil which are being used for lubrication, sealing, or internal cooling purposes. The working fluids may enter or leave the cells by the normal suction and discharge ports or may arrive or depart through various leakage paths. The volume of the control volume varies with its angular position. A comprehensive analysis [5] considers the presence of both air and oil in the cells but much can be gained from an analysis in which the presence of oil in the cells is neglected. The simplified approach is outlined in the following paragraphs. An initial estimate of the pressure, temperature, and mass of working fluid in a cell at a chosen angular position is made. Mass and energy changes are computed as the rotor turns through a small angular displacement and conditions within the cell are updated. The process is repeated for a complete rotation of the rotor and then the state of the cell contents is compared with the initially chosen values. If a close correspondence exists between the starting and finishing values the calculation is stopped, otherwise the whole process is repeated until a satisfactory convergence is achieved. Flows through the suction and discharge ports and through significant leakage paths are treated by simple orifice considerations. The ideal gas equation may be written :-

$$P_c V_c = m_c R T_c \dots\dots\dots(5.0)$$

Differentiating the above with respect to time and re-arranging using the ideal gas equation gives an equation for the cell temperature variation :-

$$\frac{dT_c}{dt} = T_c \left( \frac{1}{V_c} \frac{dV_c}{dt} + \frac{1}{P_c} \frac{dP_c}{dt} - \frac{1}{m_c} \frac{dm_c}{dt} \right) \dots\dots\dots(6.0)$$

The flow energy equation and the ideal gas law may be combined to give an equation for the cell pressure variation :-

$$\frac{dP_c}{dt} = \frac{1}{V_c} \left( (\gamma - 1) \frac{dQ}{dt} - \gamma P_c \frac{dV_c}{dt} + \gamma R \left( \sum T_i \frac{dm_i}{dt} - \sum T_o \frac{dm_o}{dt} \right) \right) \dots\dots\dots(7.0)$$

- where
- $dQ / dt$  = Heat transfer term for the control volume
  - $\sum dm_i / dt$  = Total mass transfer into the cell through the suction port and leakage paths
  - $\sum dm_o / dt$  = Total mass transfer out of the cell through the discharge port and leakage paths

The rate of change of mass inside the control volume is given by :-

$$\frac{dm_c}{dt} = \sum \frac{dm_i}{dt} - \sum \frac{dm_o}{dt} \dots\dots\dots(8.0)$$

2.3 Vane dynamics and Friction Analysis.

An analysis of the dynamic behaviour of the vanes in a sliding vane compressor is an essential step in determining the power needed to overcome frictional effects, the stability of the vanes, and likely leakage paths. Vanes are always assumed to make contact with the stator surface and at any instant the vane is assumed to be in dynamic equilibrium in a particular orientation, see for example Figure 4.0. By resolving the forces into their components acting along the vane axis and at right angles to the vane axis and by taking moments of the various forces about the centre of gravity of a vane the various contact forces may be determined. Friction forces at contact points are calculated using a Coulomb friction model where the friction force is directly proportional to the normal contact force. Different coefficients of friction are used for the contacts between the vane flanks and the vane slots and between the the vane tip and the stator surface. Some thirty possible modes of vane orientation were considered, see references [3],[4],[5], and for convenience were subdivided into six main groups :-

- Floating -
- Topping -
- Backward tilt -
- Forward tilt -
- Hard forward -
- Hard backwards-

In any mode a maximum of three contact locations is permitted.

2.3 Rotor Bearing and Rotor End Face Friction Effects.

In addition to a consideration of the frictional effects involving the sliding vanes it is also necessary to consider the effect of friction in the compressor rotor bearings and between the rotor and stator end faces. Bearing friction was estimated by assuming the existence of a uniform thickness of oil in the clearance between the rotor shafts and their surrounding housings.

The shear stress on the fluid in the bearing clearance is given by:-

$$\tau = \mu \frac{dV}{dy} = \mu \frac{\omega R_s}{y} \dots\dots\dots(9.0)$$

The torque required to overcome the force associated with the shear stress is equal to the product of the stress, the bearing surface area, and the shaft radius i.e

$$\text{Torque} = \frac{\mu \omega R_s}{y} \times 2\pi R_s L \times R_s = \frac{4\pi^2 R_s^3 N L \mu}{60y} \dots\dots\dots(10.0)$$

where L = bearing length,  $R_s$  = shaft radius, y = bearing clearance,  $\mu$  = fluid dynamic viscosity, N = rotational speed. During operation of the compressor friction is generated between the rotor end faces and the stator end plates. The magnitude of the frictional effect will depend on the clearance between the rotor end faces and the stator end plates, and the nature of the fluid which occupies this clearance. Large clearances lead to significant inter-cell leakages of the fluid being compressed whilst very small clearances are associated with high frictional effects. Assuming that the clearance between the end plates and the rotor end faces is filled with lubricating oil which gives rise to a viscous drag the frictional force may be estimated. On the assumption that the radial velocity of the lubricant in the clearance space is negligible compared with its tangential velocity the friction torque may be considered as that arising between a fixed and a rotating disc i.e

$$\text{Torque} = \frac{4\pi\mu\omega}{y}(R_r^4 - R_s^4) \quad \dots\dots(11.0)$$

Where  $R_r$  = rotor radius,  $R_s$  = shaft radius,  $\omega$  = angular velocity of rotor,  $\mu$  = dynamic viscosity,  $y$  = end face clearance

The power required to drive the compressor is found by summing the power needed to achieve the compression of the working fluid and that needed to overcome the various friction effects. The total friction power takes into account friction associated with the sliding vanes, bearing and end face frictional effects, sealing arc friction effects. Thus :-

$$\begin{aligned} \text{Total Power} &= \text{Total Friction Power} + \text{Compression Power} \\ P_{\text{TOTAL}} &= P_{\text{FRICTION}} + P_{\text{COMPRESSION}} \quad \dots\dots(12.0) \end{aligned}$$

The specific capacity, i.e the volume throughput per unit of power input ( litres / kW ) was the parameter used to quantify the compressor performance, this parameter was designated FOPT. Hence :-

$$\text{FOPT} = \frac{\text{Free air delivery (FAD)}}{P_{\text{TOTAL}}} = \frac{\text{FAD}}{P_{\text{FRICTION}} + P_{\text{COMPRESSION}}} \quad \dots\dots(13.0)$$

### 3.0 CALCULATED RESULTS

#### 3.1 General Comments on Calculated Results.

The computer model was used to predict the performance of a given sliding vane compressor having a particular set of dimensions at specified operating conditions. This procedure was then used to obtain an optimum set of dimensions for the machine at its nominal design condition, i.e that combination of dimensions which gave the highest value for the specific capacity ( the value of the parameter FOPT ) expressed in litres/kWs . Once an optimum set of dimensions had been established the simulation model was used to predict the machine performance over a range of operating conditions. Table 1 in the companion paper [6] gives the basic dimensions upon which the calculations were based. The model was also used to predict the effects of changing the number of vanes and the vane inclination when the basic rotor and stator dimensions were kept constant. A selection of results is presented in the following paragraphs.

#### 3.2 Effects of Compressor Speed and Pressure Ratio on Free Air Delivery

Figure 5(a) shows the variation of free air delivery with nominal discharge pressure and compressor speed for a machine having 6 vanes inclined at  $-10^\circ$  . The nominal suction conditions were 1.013 bar absolute and 293<sup>o</sup> K and the nominal discharge pressure varied between 7.21 and 10.66 bar absolute . Figure 5 (a) shows that the free air delivery varies virtually linearly with the rotational speed and that the operating pressure ratio has little effect on the volume of air delivered. In fact the free air delivery does diminish slightly as the discharge pressure is raised ( increased operating pressure ratio ) . This trend is clearly shown in Figure 5(a). Similar results are shown for a machine having 6 vanes inclined at  $+10^\circ$  in Figure 6(a) . The predicted variations were in accord with the corresponding experimental findings.

#### 3.3 Effects of Compressor Speed and Pressure Ratio on Shaft Input Power.

Figures 5(b), 6(b) show quite clearly that for a given machine the shaft input power depends on both the compressor speed and the operating pressure ratio. At a given speed the shaft input power increases almost linearly with increases of discharge pressure over the range of conditions employed. For a given suction and discharge pressure condition the shaft input power increases more rapidly as the rotational speed is increased. This behaviour is in accord with the argument that the vane tip frictional effects are greatly influenced by centrifugal effects which depend on the square of the rotational speed. Once again these trends were corroborated by experiment.

#### 3.4 Effects of Compressor Speed and Pressure Ratio on Specific Capacity (FOPT).

Figures 5(c), 6(c) illustrate the variation of the specific capacity (the parameter FOPT) with changes in compressor speed and operating pressure ratio. Figure 5(c) is for a machine with 6 vanes inclined at  $-10^\circ$  whilst Figure 6(c) is for a 6 vane machine with vanes inclined at  $+10^\circ$ . The basic trends are very similar. For a given operating pressure ratio the specific capacity is virtually constant over a fairly wide speed range. When the rotational speed is kept constant the specific capacity decreases slightly as the operating pressure ratio is raised. These general comments applied to machines with both forward and backward inclined vanes. The effects of vane inclination are considered in more detail in the following section.

### 3.5 Effects of Vane Inclination Upon Compressor Performance.

Figures 7(a) to 7(e) show to an enlarged scale the effects produced by variations in the vane inclination. These figures relate to a situation where all the machine dimensions are fixed. Only the vane inclination was changed. Figures 7(a) to 7(e) are for the nominal design condition with  $P_s = 1.013$  bar absolute,  $T_s = 293$  K,  $P_D = 7.91$  bar absolute, and  $N = 1450$  rev / min. Examination of Figure 7(a) shows that vane inclination has virtually no effect on free air delivery at the specified operating condition. The free air delivery remained approximately constant at 15.55 litre / s as the vane inclination was varied from  $-30^\circ$  to  $+30^\circ$ .

Figure 7(b) shows that the indicated power varies slightly with the vane inclination. This power is based on the indicated cycle work, the number of active cells (vanes) and the rotational speed. For the conditions studied the indicated power decreased from 4.56 kW at  $\sigma = -30^\circ$  to 4.535 kW at  $\sigma = +15^\circ$  before increasing again. The change in the indicated power is of the order of 0.55% of the indicated power of a zero vane inclination machine.

Figure 7(c) shows the variation of the friction power with the vane inclination and it is clearly seen that vane inclination has a noticeable effect on the friction power. The friction power is predicted to fall from 1.33 kW at  $\sigma = -30^\circ$  to 0.8 kW at  $\sigma = 0^\circ$  before increasing to 0.98 kW at  $\sigma = +30^\circ$ . Whilst Figure 7(c) shows the variation in the total friction power it really shows the effect of vane inclination upon vane tip and vane flank friction since end face and bearing conditions are essentially unchanged.

Figure 7(d) combines the two previous figures to show the variation of the compressor input power with vane inclination. The figure shows a minimum total power input of 5.35 kW for a vane inclination of approximately  $2.5^\circ$ .

Figure 7(e) combines the results of Figures 7(a) and 7(d) to show the variation of the parameter FOPT, the specific capacity, with vane inclination. The specific capacity increases from 2.46 litres / kW at  $\sigma = -30^\circ$  to 2.74 litres / kW at a vane inclination of  $+5^\circ$  before decreasing to 2.65 litres / kW at  $\sigma = +30^\circ$ . The variation in FOPT is associated wholly with the variation of the friction power since by comparison the effects of vane inclination upon the free air delivery and the indicated power are negligibly small. A machine fitted with forward inclined vanes is predicted to perform better than a machine fitted with correspondingly backward inclined vanes.

### 3.6 Effect of the Number of Vanes Upon Compressor Performance

The computer model was used to demonstrate what would be the effect of varying the number of vanes upon the predicted compressor performance. In this comparison which is shown in Figure 8 with the exception of the number of vanes or the vane inclination all other design parameters and operating conditions were fixed. Figure 8 shows that reducing the number of vanes from 8 to 6 results in an increase in specific capacity. This is not too surprising since fewer vanes implies less vane friction. These findings accord with the work of Ooi [4] who predicted theoretically that reducing the number of vanes brings significant benefits and whilst a further reduction to 4 vanes is clearly feasible its benefits would begin to be countered by the increased internal leakage effects which might be expected.

## 4.0 CONCLUSIONS

The authors have demonstrated that they have developed a comprehensive computer model which is able to predict the behaviour of a rotary sliding vane air compressor. The model is able to be used as a design tool so that a designer may now take into consideration the effects of changing many of the parameters which are at his disposal.

The model has successfully predicted the effects of changing the operating conditions of a given machine and has demonstrated that changes in the vane inclination have an effect upon compressor performance.

Whilst the paper has shown that machines fitted with vanes having a small forward inclination ( $+5^\circ$ ) have an enhanced specific capacity the increase in specific capacity compared to that of a machine fitted with radially aligned vanes is extremely small and would not justify the increased manufacturing costs associated with inclined vanes.

### 5.0 REFERENCES

1. Peterson, C. R. and McGahan, W. A. "Thermodynamic and Aerodynamic Analysis Methods for Oil Flooded Sliding Vane Compressors." Proceedings of the 1972 Purdue Compressor Technology Conference. pp 1 - 8.
2. Pandeya, P. and Soedel, W. "Rolling Piston Type Rotary Compressors with Special Attention to Friction and Leakages." Proceedings of the 1978 Purdue Compressor Technology Conference. pp 209 - 218.
3. Chang, K. Y. "A Theoretical and Experimental Study of an Oil-Flooded Rotary Sliding Vane Compressor." Ph.D. Thesis 1983, Vols. 1 and 2, University of Strathclyde.
4. Ooi, K. T. "Geometrical Optimization of Rotary Sliding Vane Air Compressors." Ph.D. Thesis 1989, University of Strathclyde.
5. Mkumbwa, M. H. "Simulation and Geometrical Optimization of Radial and Non-radial Rotary Sliding Vane Compressors." Ph.D. Thesis 1995, University of Strathclyde.
6. Tramschek, A. B. and Mkumbwa, M. H. "Experimental Studies of Non-radial Rotary Sliding Vane Compressors During Steady State Operation." Proceedings of the 1996 International Compressor Engineering Conference at Purdue.

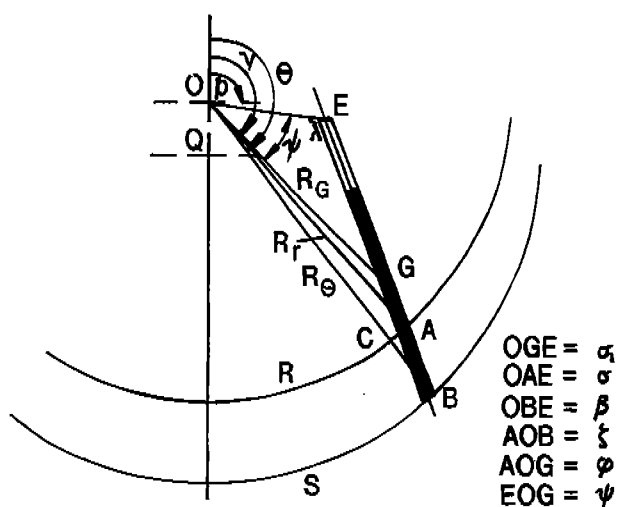


FIG. 1.0 FORWARD INCLINED VANE.

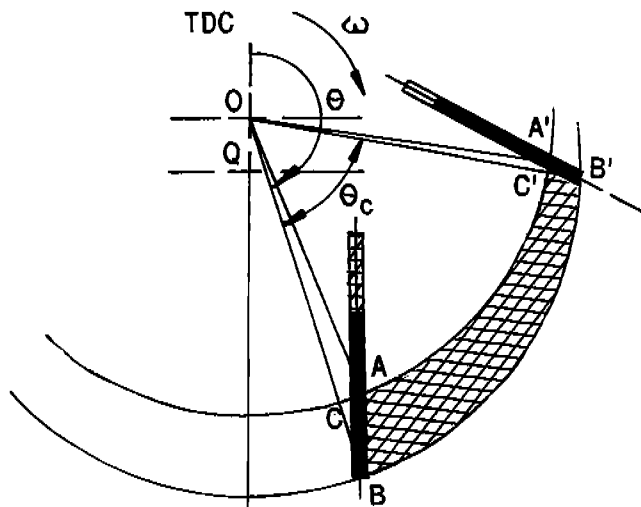


FIG. 2.0 CELL CROSS-SECTIONAL AREA.

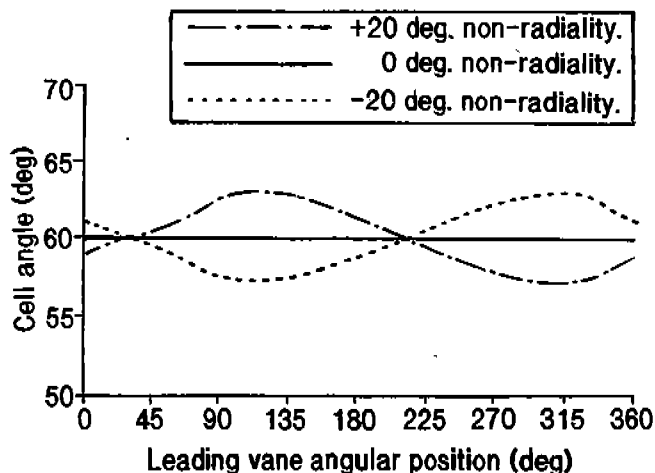


FIG. 3.0 VARIATION OF CELL ANGLE WITH LEADING VANE ANGULAR POSITION.

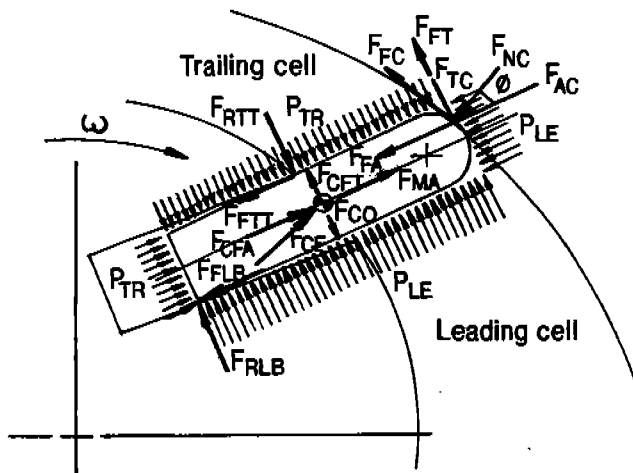


FIG. 4.0 (BACKWARDS TILT) GENERAL FORCE SYSTEM ON THE VANE.

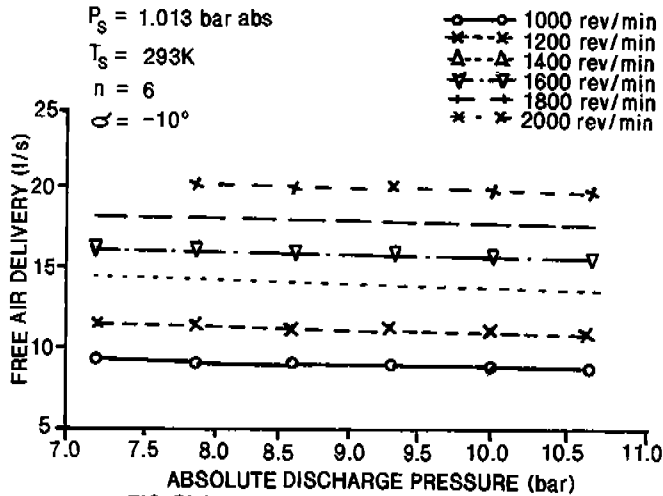


FIG. 5(a) VARIATION OF FREE AIR DELIVERY WITH DISCHARGE PRESSURE

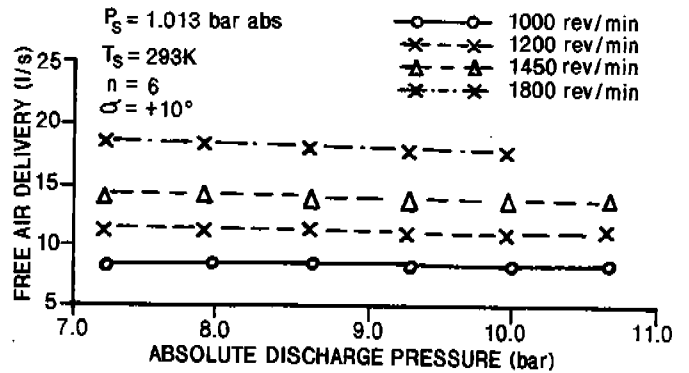


FIG 6(a) VARIATION OF FREE AIR DELIVERY WITH DISCHARGE PRESSURE

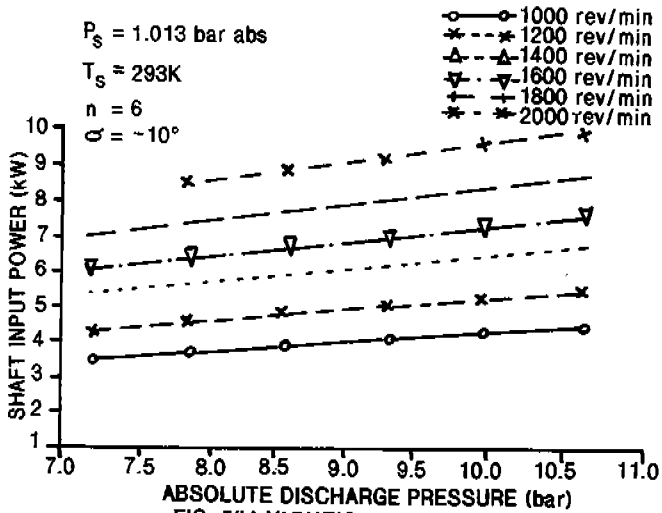


FIG. 5(b) VARIATION OF SHAFT INPUT POWER WITH DISCHARGE PRESSURE

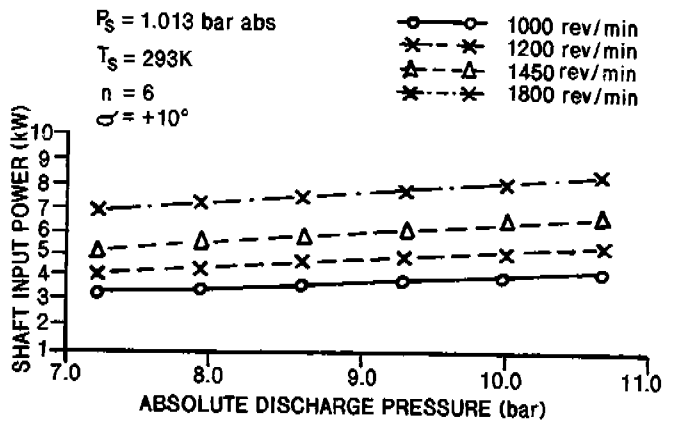


FIG 6(b) VARIATION OF SHAFT INPUT POWER WITH DISCHARGE PRESSURE

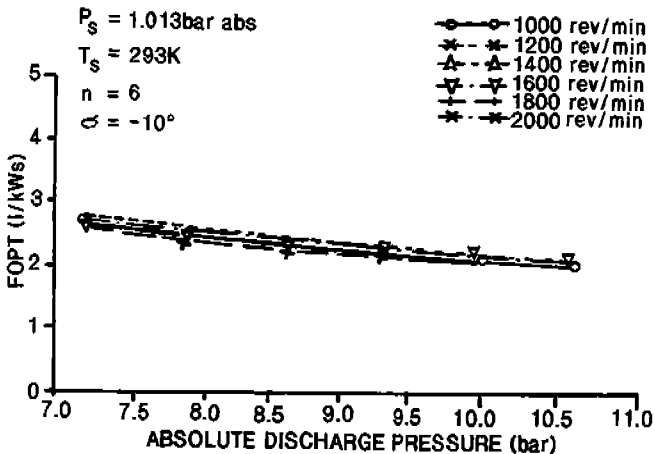


FIG. 5(c) VARIATION OF VOLUME THROUGHPUT WITH DISCHARGE PRESSURE

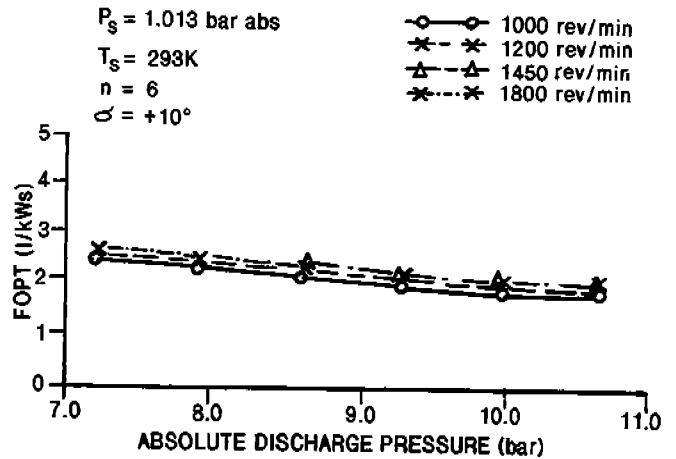


FIG 6(c) VARIATION OF VOLUME THROUGHPUT WITH DISCHARGE PRESSURE



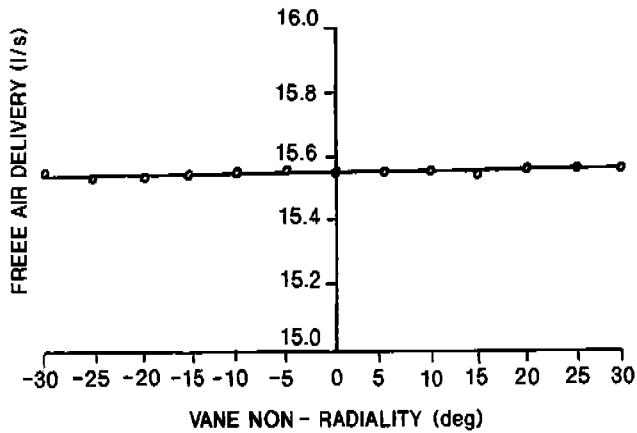


FIG. 7(a) VARIATION OF FREE AIR DELIVERY WITH VANE NON - RADIALITY

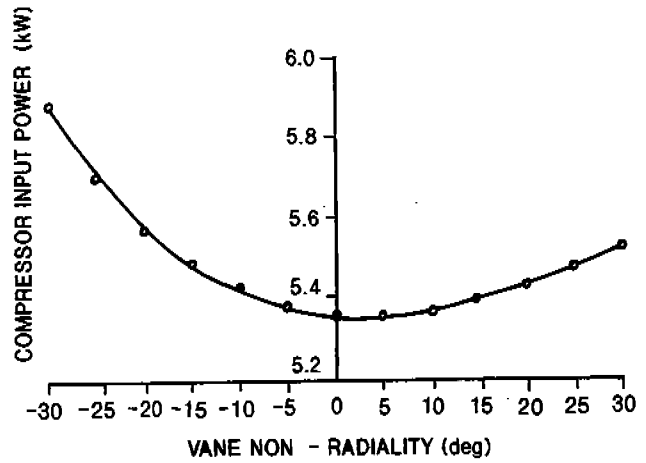


FIG. 7(d) VARIATION OF COMPRESSOR INPUT POWER WITH VANE NON - RADIALITY

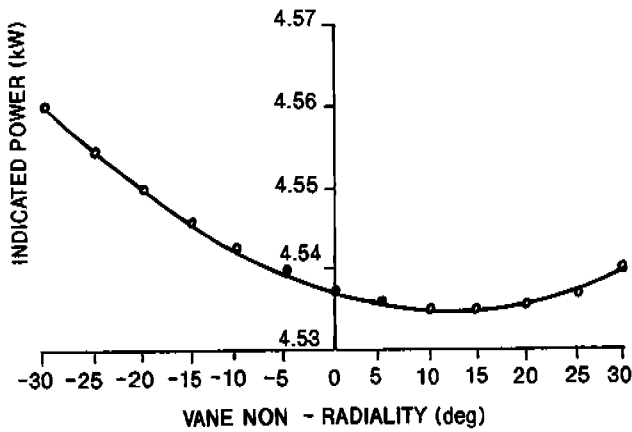


FIG. 7(b) VARIATION OF INDICATED POWER WITH VANE NON - RADIALITY

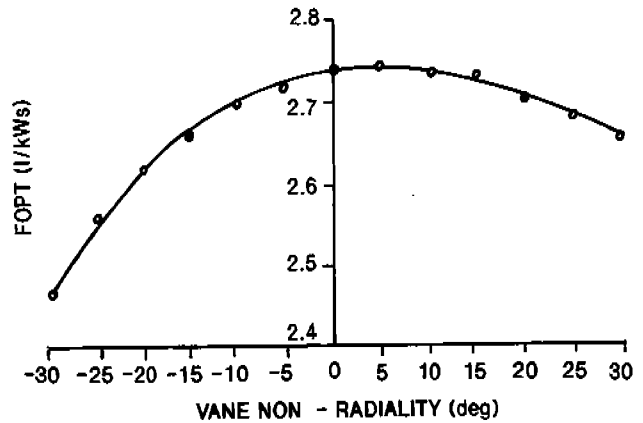


FIG. 7(e) VARIATION OF THROUGHPUT WITH VANE NON - RADIALITY

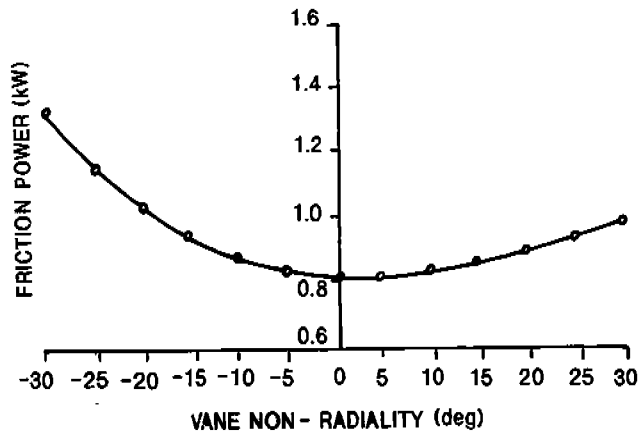


FIG. 7(c) VARIATION OF FRICTION POWER WITH VANE NON - RADIALITY

$P_s = 1.013 \text{ bar abs}$        $P_d = 7.91 \text{ bar abs}$   
 $T_s = 293\text{K}$                  $N = 1450 \text{ rev/min}$

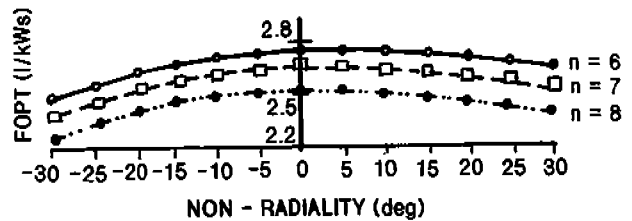


FIG. 8 VARIATION OF VOLUME THROUGHPUT WITH NON RADIALITY AND NUMBER OF VANES